Secreted MMP9 promotes angiogenesis more efficiently than constitutive active MMP9 bound to the tumor cell surface

Emilia Mira, Rosa Ana Lacalle, José María Buesa, Gonzalo González de Buitrago, Sonia Jiménez-Baranda, Concepción Gómez-Moutón, Carlos Martínez-A and Santos Mañes*

Department of Immunology and Oncology, Centro Nacional de Biotecnología/CSIC, Universidad Autónoma de Madrid, Cantoblanco, E-28049 Madrid, Spain

*Author for correspondence (e-mail: smanes@cnb.uam.es)

Accepted 3 December 2003
Journal of Cell Science 117, 1847-1856 Published by The Company of Biologists 2004
doi:10.1242/jcs.01035

Summary

Association of matrix metalloprotease 9 (MMP9) to the cell membrane is considered important in tumor growth and angiogenesis. To dissect this regulatory mechanism, we generated raft and non-raft MMP9 chimeras to force membrane expression in the MCF-7 human breast carcinoma cell line. MMP9 targeting to non-raft cell surface domains rendered a constitutive active membrane MMP9 form, suggesting a contribution by the lipid environment in MMP activation. We generated human breast cancer xenograft models using MCF-7 cells overexpressing secreted and membrane-anchored MMP9. The non-raft MMP9 chimera was constitutively active at the cell membrane in xenografts, but this activation did not correlate with an increase in MMP9-induced angiogenesis. Capillary number and vessel perimeter were specifically increased only in tumors overexpressing wild-type MMP9 (the secreted form); this increase was inhibited when tumors were induced in doxycycline-treated mice. Xenografts from tumor cells overexpressing wild-type MMP9 showed increased vascular endothelial growth factor (VEGF)/VEGFR2 receptor association, which was also dependent on MMP9 activity. These observations indicate that membrane location can influence MMP9 activity in vitro and in vivo, and confirm the relevance of stromal-associated, but not tumor-bound MMP9 in mediating tumor-induced angiogenesis.

Supplemental data available online

Key words: Metalloprotease, Tumor growth, Angiogenesis, Lipid rafts, Membrane targeting

Introduction

Increasing evidence suggests that matrix metalloproteases (MMP), a family of multidomain, zinc-containing neutral endopeptidases, contribute to the formation of a microenvironment that promotes tumor growth during early stages of tumorigenesis (Egeblad and Werb, 2002; Overall and López-Otín, 2002). The MMPs have traditionally been considered proteolytic enzymes for extracellular matrix (ECM) components, although it is now recognized that MMPs also cleave 'non-matrix' molecules, including growth factors, growth factor binding proteins, cytokines, chemokines, adhesion and death receptors as well as other proteinases, modifying their biological activity (Mañes et al., 1997; Mañes et al., 1999a; Wilson et al., 1999; Bergers et al., 2000; McQuibban et al., 2000; Yu and Stamenkovic, 2000; Fingleton et al., 2001; Rodríguez-Manzaneque et al., 2001; McQuibban et al., 2002). These MMP degradative activities may augment or reduce proliferation, survival and migration of both tumor and stromal cells. MMP-induced release of biological mediators from the ECM surrounding a tumor may thus constitute a system by which neoplastic and stromal cells communicate.

MMP activity is grossly regulated at the transcriptional level; it has nonetheless been suggested that MMP function is fine-tuned by recruitment and/or confinement of MMP activity to the cell surface (Fridman, 2003). Plasma membrane association is not restricted to transmembrane and glycosylphosphatidylinositol (GPI)-linked MMP, since secreted MMP forms including MMP-1, -2, -7, -9, -13 and -19 (Brooks et al., 1996; Mazzieri et al., 1997; Guo et al., 2000; Yu and Woessner, 2000; Fridman, 2003) also bind to the cell surface. MMP membrane binding is a mechanism that proteolyzes cell-associated substrates, activates and/or concentrates MMP activity in discrete areas, preserves MMP activity from inhibition, and silences MMP activity. In the case of MMP9, high affinity binding has been reported to MMP9 substrates such as type IV collagen α2 chain (Olson et al., 1998; Toth et al., 1999) and the intercellular adhesion molecule (ICAM) 1 (Fiore et al., 2002), to docking proteins such as β1 integrin (Partridge et al., 1997) and the hyaluronan receptor CD44 (Bourguignon et al., 1998; Yu and Stamenkovic, 2000), and to the scavenger receptor LRP (low density lipoprotein receptor-related protein) (Hahn-Dantona et al., 2001). It has nonetheless been proposed that membrane-bound MMP9 represents only a very small fraction of the enzyme and that the MMP9 biologically relevant for tumor development is the secreted form (Ramos-DeSimone et al., 1999).

MMP regulation at the cell surface may be more complex as

the plasma membrane is composed of distinct lipid domains that organize proteins functionally in the bilayer. One of these microdomain types, termed rafts, is formed by glycosphingolipid (GSL), sphingomyelin and cholesterol packaging in the plasma membrane (Simons and Toomre, 2000). Because of this lipid composition, rafts are membranes in a liquid-ordered conformation that embed specific proteins, such as GPI-anchored and double-acylated cytoplasmic proteins, whereas other proteins are selectively excluded from these microdomains. GPI-anchored MMP17 and MMP25 thus presumably partition in rafts, and MMP2 and MMP14 (MT1-MMP) association with rafts is suggested, based on biochemical and cytological data (Annabi et al., 2001; Puyraimond et al., 2001).

Since rafts function as devices that control membrane protein-protein interactions (Mañes et al., 2001; Mañes et al., 2003b), MMP may be activated or inhibited as a result of raft association. MMP2 and its activator MMP14 partition in rafts, suggesting that MMP activators can concentrate in these domains (Puyraimond et al., 2001). Rafts may also accumulate MMP inhibitors such as the GPI-anchored RECK (reversion-inducing cysteine-rich protein with Kazal motifs) (Egeblad and Werb, 2002). Rafts are distributed asymmetrically at the front of moving tumor cells and epithelial cells during cell migration (Mañes et al., 1999b; Zhao et al., 2002; Mañes et al., 2003a). MMP association with rafts may thus focus proteolytic activity to specific cell areas during cell migration; for example, MMP14 location at the leading cell edge requires its association with raft protein CD44 (Mori et al., 2002). Again, as rafts are probably enriched in RECK, MMP inclusion in these microdomains might be a local mechanism to silence their proteolytic activity.

To study the role of MMP membrane localization in tumor progression, we forced membrane raft and non-raft expression of secreted MMP9 in the MCF-7 human breast carcinoma cell line, which expresses very low MMP9 levels. The data indicate that although the non-raft MMP9 chimera was constitutively active in the MCF-7 cell membrane, secreted wild-type MMP9 promoted tumor cell invasion, tumor growth and ‘angiogenic switch’ more efficiently than the membrane-anchored MMP9 forms. These results highlight the relevance of pericellular regulatory mechanisms that coordinate expression of a specific MMP with its activation and physical location.

Materials and Methods

Recombinant MMP9 chimeras and cell transduction

A GPI consensus sequence, and the transmembrane and juxtamembrane low-density lipoprotein receptor (LDLR) were rescued from pGFP-GPI and pLGFP-GT46 (P. Keller, Max Planck Institute of Cell Biology and Genetics, Dresden, Germany) as described (del Real et al., 2002), and cloned in-frame at the 3′ end of the MMP9 wild-type (MMP9-wt) sequence. MMP9-GPI, MMP9-LDL and MMP9-wt were subcloned in the bicistronic plasmid pRV-IRES-GFP (Mira et al., 2001) to obtain recombinant retroviruses used to transduce MCF-7 and DU-145 cells. Green fluorescent protein-expressing cells were selected by fluorescence-activated cell sorting. The coding sequences for MMP9-GPI and MMP9-LDL were also cloned in the plasmid pBacPAK8 (Clontech) to produce recombinant MMP9 chimeras in the baculovirus system. Recombinant proteins were affinity chromatography purified from insect cell extracts using gelatin-Sepharose (Amersham Pharmacia Biotech).

Cell fractionation

Transduced cells were disrupted with 25- and 30-gauge needles in TNE buffer (50 mM Tris, pH 7.4, 150 mM NaCl, 5 mM EDTA and protease inhibitors). Membrane and cytosolic fractions were obtained by centrifugation (166,000 ***g***, for 1 hour, at 4°C) in a 30-25% OptiPrep gradient (Nycomed-Pharma, Oslo, Norway). Detergent-resistant membranes (DRM) were isolated using a flotation gradient after Triton X-100 extraction, as described previously (Mañes et al., 1999b). As a quality control of flotation gradients, normalized protein amounts for each fraction were analyzed with anti-transferrin receptor (TfR; Zymed, San Francisco, CA) and anti-VIP21 (CAV-1; Santa Cruz Biotech, Santa Cruz, CA) in western blots.

Colocalization studies

Transfected MCF-7 cells plated on vitronectin were incubated (30 minutes, 12°C) with an anti-MMP9 polyclonal antibody (Calbiochem) followed by Cy3-labeled anti-rabbit antibody (Jackson ImmunoResearch; 30 minutes; 12°C). FITC-cholera toxin β-subunit (CTx; 6 μg/ml; Sigma) was added during the last 10 minutes to detect ganglioside monosialic acid 1 (GM1). Cells were fixed with 3.7% paraformaldehyde (5 minutes on ice) and methanol (10 minutes, –20°C), mounted in Vectashield (Vector, Burlingame, CA) and analyzed by confocal microscopy (Leica).

Tumor xenograft models and immunohistochemistry

Cells (5×10^6) were injected subcutaneously into each flank of female SCID mice pretreated with 17α-ethynyl estradiol (1 μg/ml; Sigma) in drinking water for 1 week before cell injection and throughout the experimental period. In some experiments, mice were also pretreated with doxycycline (0.4 mg/ml; Sigma) in drinking water (Pozzi et al., 2002). Tumor volume was estimated according to the formula $(W^2 \times L)/2$, where W is width and L is length of the tumor mass. Primary tumors were removed after 14-18 weeks and snap-frozen in Tissue Freezing Medium (Jung, Nussloch, Germany) for histology, or frozen and mechanically disrupted in RIPA buffer to prepare cell lysates. Sera were collected from mice and diluted 2.5-fold for gelatin zymography.

Frozen tumor sections (6 μm) were acetone-fixed and stained with Hematoxylin-Eosin, anti-mouse CD31 (PECAM-1; Pharmingen), GV39M mAb (Brekken et al., 1998), or anti-VEGF mAb Ab-3 (NeoMarkers), followed by appropriate Cy3-conjugated secondary antibodies. CD31-positive structures were used to determine microvessel density and perimeter, respectively, as the number of vascular profiles (magnification ×200) and total positive stained area (×400), using Adobe Photoshop.

MMP9 activity assays

MMP9 activity was analyzed in membrane and cytosolic fractions, serum samples or tumor extracts by gelatin zymograms as described previously (Quesada et al., 1997). MMP9 activity in tumor extracts was quantitated by incubating extracts in 50 mM Tris, pH 7.4, 150 mM NaCl, 10 mM $CaCl_2$ and 0.1% Brij-35 (3 hour, 37°C) with 50 μg/ml FITC-gelatin (DQ-gelatin, Molecular Probes, Eugene, OR, USA), which yields fluorescence after proteolytic cleavage. Values represent the fluorescence increment after subtraction of background fluorescence from a blank well without protein.

Cell surface MMP9 activity was quantified using the fluorogenic peptide M-2055 (Bachem, Bubendorf, Switzerland) as a substrate (Mira et al., 1999). For in situ zymography, vitronectin-plated cells were incubated with DQ-gelatin (40 μg/ml, 2 hours, 37°C). When included, GM6001 (100 μM; Chemicon) was added 15 minutes before substrate addition. Cells were washed with PBS, fixed with 1% paraformaldehyde, mounted in Vectashield and analyzed by confocal laser microscopy. To analyze tumor samples, unfixed 8 μm frozen

sections were incubated with DQ-gelatin (20 μg/ml, 30 minutes, 37°C) and, after substrate removal, mounted without washing in Vectashield.

Activation of MMP9 chimeras

RIPA extracts from MCF-7 cells overexpressing MMP9-GPI and MMP9-LDL were partially purified by size-exclusion chromatography. Fractions enriched in each protein were incubated (16 hours, 37°C) with α2-macroglobulin (α2-MG; 1 μg/μl; Calbiochem) alone or with 4-aminophenylmercuric acetate (APMA; 1 mM), and analyzed by gelatin zymography.

MCF-7 cells overexpressing MMP9-GPI and MMP9-LDL were incubated (16 hours, 37°C) in Batimastat (BB-94; 1 μM), 1 μM GM6001, aprotinin (20 μg/ml; Sigma), neutralizing anti- urokinase-type plasminogen activator (uPA) mAb (Chemicon), plasminogen activator inhibitor (PAI)-1 (0.4 μM; Calbiochem), or irrelevant antibodies and DMSO as controls. Lysates (1-5 μg) from treated cells were analyzed by gelatin zymography.

Intravasation assays

For intravasation, 2×10^6 cells were inoculated onto chorioallantoic membranes (CAM) of 9-day-old chick embryos. After 48 hours, human Alu DNA sequences were quantified by real-time PCR (Mira et al., 2002).

EIA of tumor extracts

Mouse or human vascular endothelial growth factor (VEGF), human basic fibroblast growth factor (bFGF), human transforming growth factor (TGF) β and human interleukin (IL) 8 levels in tumor extracts (50-200 μg) were measured by enzyme immunoassay (R&D Systems, Minneapolis, MN).

Results

MMP9 targeting to raft and non-raft membranes

To force MMP9 expression at the cell membrane, we fused a GPI consensus sequence (MMP9-GPI) or the transmembrane LDLR domain (MMP9-LDL) to the MMP9 C terminus (Fig. 1A). Zymographic analysis of membrane and cytosolic fractions from MCF-7 cells transfected with these chimeras confirmed that these tags effectively targeted MMP9 to the plasma membrane (Fig. 1B). We nonetheless detected no substantial membrane association of the soluble MMP9 wild-type form (MMP9-wt), which was secreted mainly into the medium (Fig. 1C). A fraction of MMP9-GPI was also recovered in the conditioned medium, although it represented less than 0.1% of the total chimera expressed. MMP9 was not detected in mock-transfected cell extracts, and was almost undetectable in the medium (Fig. 1B,C).

Raft-associated proteins can be isolated in the detergent-resistant membrane (DRM) fraction at the top of density gradients, whereas non-raft membrane and cytosolic proteins partition in the detergent-soluble fraction at the bottom. Only MMP9-GPI co-purified with the raft marker caveolin-1 in DRM; the MMP9-LDL chimera and MMP9-wt co-fractionated with the non-raft marker transferrin receptor (TfR) (Fig. 1D). In confocal analysis, MMP9-GPI colocalized extensively with cholera toxin (CTx), which binds to the raft ganglioside GM1 (Fig. 1Ea), indicating association with rafts. MMP9-LDL did not colocalize with CTx (Fig. 1Eb), suggesting that this chimera partitioned to non-raft membranes. Cells expressing

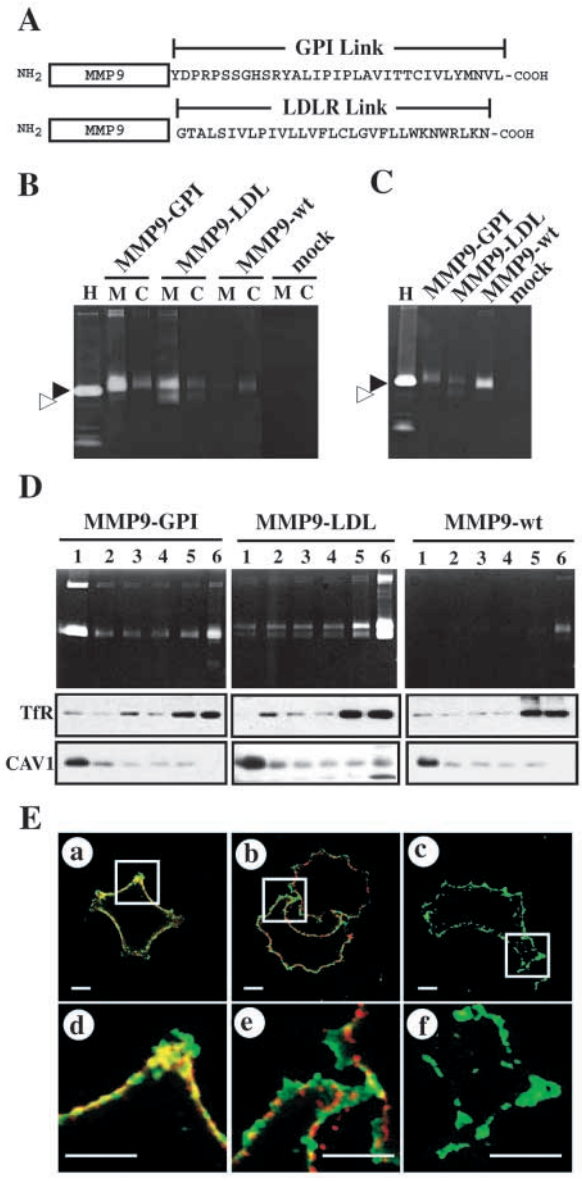

Fig. 1. Partitioning of MMP9 chimeras into distinct membrane domains. (A) Schematic representation of the MMP9-GPI and the MMP9-LDL chimeras. (B) Gelatinolytic activity in membrane (M) and cytosolic (C) fractions isolated from MMP9-GPI-, MMP9-LDL-, MMP9-wt and mock-transfected MCF-7 cells. ProMMP9 (solid arrowhead) and MMP9 (open arrowhead) activity in HT-1080 conditioned medium (H). (C) Gelatinolytic activity in conditioned medium from the same cells as in B after 24 hours of serum depletion. (D) MCF-7 cells expressing all MMP9 forms were fractionated in flotation gradients and analyzed by zymography. Fractions 1 and 6 represent the top and the bottom of the gradient, respectively. The same fractions were analyzed by western blot with anti-TfR and anti-VIP21 (CAV-1) as controls for non-raft- and raft-associated proteins, respectively. (E) Confocal microscopy of MMP9-expressing cells stained with cholera toxin β-subunit (green) and anti-MMP9 antibody (red); yellow staining indicates colocalization of the molecules. The two-color overlays show representative cells for (a) MMP9-GPI, (b) MMP9-LDL and (c) MMP9-wt (n=50). The boxed regions in these images are enlarged in d, e and f, respectively. Scale bar, 10 μm. Single-color images are available: Fig. S1, http://jcs.biologists.org/supplemental/

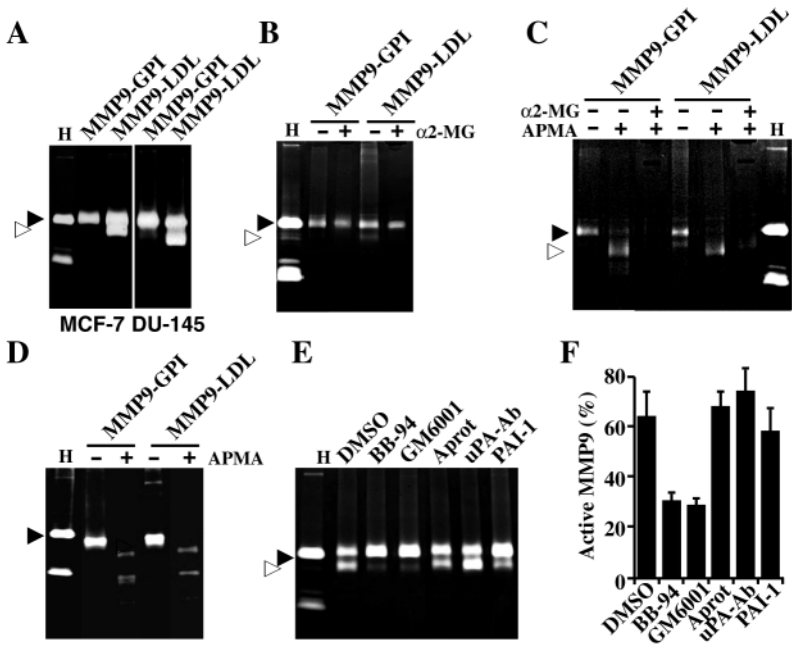

Fig. 2. Non-raft proMMP9 is processed at the cell surface. (A) Gelatinolytic activity in MMP9-GPI and MMP9-LDL-expressing MCF-7 and DU-145 cell extracts. (B) MMP9-GPI and MMP9-LDL, partially purified from MCF-7 cell extracts, were incubated alone (–) or with α2-MG (+), then analyzed by gelatin zymography. (C) Samples in B were incubated alone or with α2-MG in the presence (+) or absence (–) of 4-aminophenylmercuric acetate (APMA) before gelatin zymography. (D) Insect cell-derived MMP9-GPI and MMP9-LDL were in vitro processed with APMA before gelatin zymography. (E) MCF-7 cells expressing MMP9-LDL were incubated with DMSO, BB-94, GM6001, aprotinin, anti-uPA or PAI-1, and cell extracts were analyzed by gelatin zymography. In all zymograms, solid and open arrowheads indicate the migration of proMMP9 and MMP9 forms, respectively. Activity is also shown in HT-1080 medium (H). (F) Zymograms in E were analyzed by densitometry and the quotient between the intensities obtained for MMP9 and proMMP9 calculated. The values represent mean±s.d. of results obtained in two independent experiments.

MMP9-wt stained weakly with anti-MMP9 antibody (Fig. 1Ec), again indicating that MMP9-wt does not bind extensively to the MCF-7 cell surface (see Fig. S1, http://jcs.biologists.org/supplemental/ for single color images).

The non-raft MMP9-LDL chimera is activated at the plasma membrane

MMP9-LDL was characterized as two gelatinolytic bands in zymographic analysis, whereas raft-associated MMP9-GPIs appeared as a single band (Fig. 1B,D). Similar results were obtained when MMP9-LDL and MMP9-GPI were expressed in the prostate cell line DU-145 (Fig. 2A), showing that the specific gelatinolytic pattern for raft and non-raft chimeras was not restricted to MCF-7 cells. Incubation of partially purified MMP9-LDL with α2-macroglobulin (α2-MG) resulted in specific loss of low molecular mass gelatinolytic activity (Fig. 2B), indicating that this band corresponds to an active protease form. MMP9-GPI and high molecular mass MMP9-LDL gelatinolytic bands were unaffected by α2-MG incubation. These results suggest that non-raft MMP9-LDL is activated in the membrane, whereas MMP9-GPI remains mostly as a proform.

Partially purified MMP9-LDL and MMP9-GPI (Fig. 2C), as well as baculovirus-produced recombinant proteins (Fig. 2D), were activated similarly after 4-aminophenylmercuric acetate (APMA) treatment; as predicted, the APMA-processed purified forms were sequestered by α2-MG. These results suggest that the C-terminal tags that anchor MMP9 to raft and non-raft membranes do not influence their in vitro processing.

To study the mechanisms involved in MMP9-LDL activation at the plasma membrane, we incubated MCF-7 cells expressing this chimera with several MMP and serine protease inhibitors. The MMP inhibitors BB-94 and GM6001 inhibited MMP9-LDL processing (Fig. 2E,F), which was unaffected by aprotinin, neutralizing anti-uPA monoclonal antibody (mAb), or PAI-1, suggesting that an MMP-dependent pathway is responsible for MMP9-LDL activation at the cell surface.

The active MMP9-LDL chimera does not enhance tumor invasion

The α2-MG entrapment assay suggested the presence of active MMP9-LDL at the cell surface. Confirming this hypothesis, MMP9-LDL-expressing MCF-7 cells showed enhanced M-2055 substrate degradation compared to mock-transfected, MMP9-wt or MMP9-GPI-expressing forms (Fig. 3A). Incubation of MMP9-GPI-expressing MCF-7 cells with DQ-gelatin to visualize MMP activity in situ resulted in punctuate cytosolic staining, which was more intense around the nucleus; little or no membrane staining was observed (Fig. 3Ba). A similar pattern was seen in mock-transfected or MMP9-wt-expressing cells (not shown). In MMP9-LDL-expressing cells, however, we detected clear staining at the plasma membrane (Fig. 3Bb), which was lost after pre-incubation of cells with the MMP inhibitor GM6001 (Fig. 3Bc). This result indicates that specific membrane staining in MMP9-LDL cells is the consequence of MMP activity. The cytosolic staining found in all cell types is probably due to non-specific uptake of DQ-gelatin, which is cleaved in internal cell compartments by GM6001-resistant gelatinolytic proteases.

We analyzed whether constitutive active MMP9-LDL provided a selective advantage for ECM invasion. Vitronectin-coated transwell-based chemotaxis analyses of mock-transfected, MMP9-wt, MMP9-GPI and MMP9-LDL-expressing MCF-7 cells to IGF-I, a chemoattractant for these cells (Mira et al., 1999; Mira et al., 2001), showed no significant differences among cells expressing the distinct MMP9 forms (not shown). In the chick embryo CAM intravasation model (Kim et al., 1998; Mira et al., 2002), MMP9-wt-expressing MCF-7 cells showed a higher intravasation capacity than mock-transfected, MMP9-GPI or MMP9-LDL-expressing cells (Fig. 3C; $P<0.05$, Kruskal-

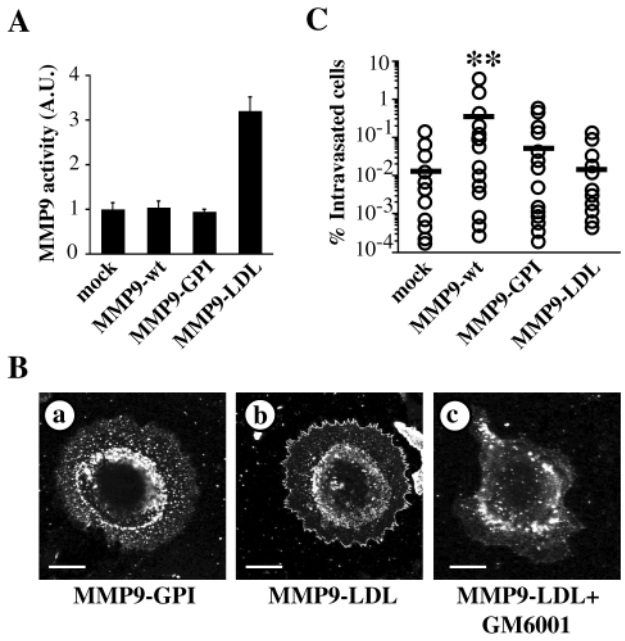

Fig. 3. Tumor invasion is not enhanced by cell surface MMP9 activity. (A) Cell surface-associated MMP9 activity was measured using the fluorogenic substrate M-2055 in intact MCF-7 cells transfected with the MMP9 forms. The fluorescence increment in mock-transfected cells was considered as 1. Data represent mean±s.e.m. of triplicates in one representative experiment of three performed. (B) MMP9-GPI-expressing (a) and MMP9-LDL-expressing (b) MCF-7 cells were incubated with DQ-gelatin and in situ gelatin degradation analyzed by confocal microscopy. Specificity was determined by preincubation of cells with GM6001 (c). Scale bar, 10 μm. (C) Tumor cell intravasation was evaluated by quantitative PCR of human DNA purified from CAM inoculated with MMP9-expressing MCF-7 cells. Data represent the percentage of intravasated human cells in each sample (mock n=21, MMP9-wt n=18, MMP9-GPI n=27 and MMP9-LDL n=22). Mean values for mock transfected, MMP9-wt-, MMP9-GPI- and MMP9-LDL-expressing MCF-7 cells were 0.013, 0.368, 0.057 and 0.016%, respectively (**P<0.05).

Wallis test). These results suggest that constitutive MMP9 activity at the tumor cell surface does not confer greater invasive capacity, although increased MMP9 levels in the tumor cell microenvironment may contribute to this process.

MMP9 localization affects angiogenesis of tumor xenografts

We analyzed tumor growth after injecting mock-transfected, MMP9-wt, MMP9-GPI or MMP9-LDL-expressing MCF-7 cells into estradiol-treated immunodeficient mice. Tumor incidence was unaffected by MMP9 overexpression or localization (Fig. 4A). MMP9-wt-expressing cells generated larger tumors than mock-transfected, MMP9-GPI or MMP9-LDL-expressing counterparts (Fig. 4B); these differences in tumor volume were statistically significant by 13 weeks post-inoculation (P<0.05, Student-Newman-Keuls test). Cell proliferation was equivalent, however, in mock-transfected, MMP9-wt, MMP9-GPI or MMP9-LDL xenografts, as

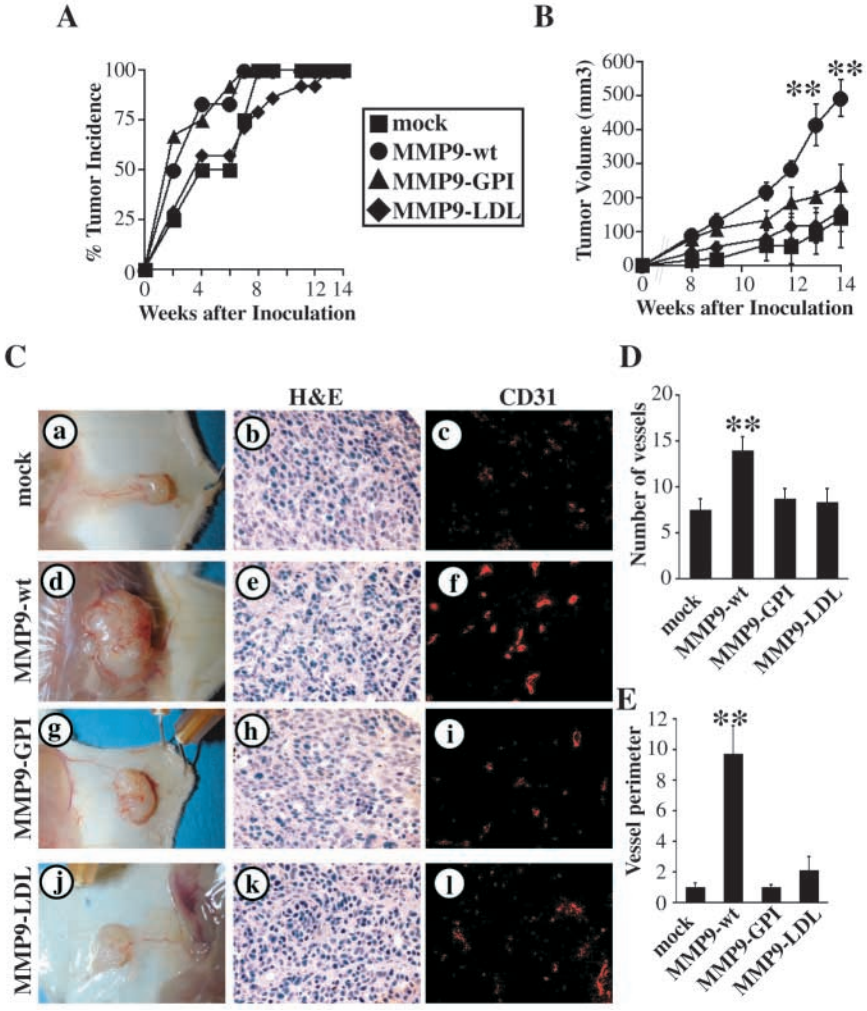

Fig. 4. Soluble MMP9 enhances tumor growth and angiogenesis. Female BALB/c-SCID mice received subcutaneous injections in both flanks of mock transfected or MMP9-expressing MCF-7 cells. (A) Tumor incidence was calculated as the percentage of palpable tumors per number of injection sites. (B) Tumor size was monitored weekly and tumor growth kinetics over a 14-week period was represented as mean tumor volume±s.e.m. (n=8, in all cases; **P<0.05). (C) Tumor vascular profile was evaluated by macroscopic observation (a,d,g,j), Hematoxylin-Eosin staining (b,e,h,k; magnification ×400) and blood vessel staining with anti-CD31 antibody (c,f,i,l; magnification ×200). (D) Blood vessel number was quantified in tumor sections stained with anti-CD31 (**P<0.05). (E) Vascular perimeter was estimated as the percentage of CD31-stained area per field. The value obtained in sections from mock-transfected tumors was considered as 1 (**P<0.05).

analyzed by tumor section staining with Ki67 antibody (not shown).

Macroscopic examination of tumors showed enhanced vascularization of MMP9-wt xenografts compared to those from mock-transfected or membrane-associated MMP9-expressing cells (Fig. 4C, first column). Blood vessel staining with anti-CD31 antibody (Fig. 4C, third column) confirmed increased angiogenesis in MMP9-wt xenografts. Tumors derived from MMP9-wt-expressing cells showed enhanced microvessel density (Fig. 4D; $P<0.05$, Student-Newman-Keuls test) and vessel perimeter (Fig. 4E; $P<0.05$, Student-Newman-Keuls test) compared with those from mock-transfected, MMP9-GPI or MMP9-LDL-expressing cells. Since no differences in vessel density or perimeter were observed in mock-transfected, MMP9-GPI or MMP9-LDL xenografts, the results suggest that tumor angiogenesis is specifically enhanced by MMP9-wt overexpression, but not by overexpression of membrane-associated MMP9 forms.

Enhanced MMP9-wt tumor angiogenesis requires MMP9 activity

We analyzed protease levels in tumors from all MCF-7 MMP9-expressing cells. Gelatin zymography of total cell extracts confirmed increased proMMP9 expression in the transfected xenografts compared to mock-transfected tumors (Fig. 5A). In addition to proMMP9, we detected the active MMP9 form in MMP9-wt and MMP9-LDL-derived tumors, but not in MMP9-GPI-expressing tumors. Notably, all xenografts, including those from mock-transfected cells, showed two faint gelatinolytic bands that comigrated with the pro- and active MMP2 forms in HT-1080-conditioned medium (Fig. 5A); band intensity was unaffected by MMP9 expression or cell location.

In situ zymography showed strong gelatinolytic activity delineating the cell contour in MMP9-LDL-derived xenografts, which contrasted with the weak activity in mock-transfected, MMP9-wt and MMP9-GPI xenografts (Fig. 5B). This is consistent with the membrane-associated MMP9 activity in MMP9-LDL-expressing cells. This staining pattern may nonetheless overestimate MMP9-LDL gelatinolytic activity compared to the diffuse staining of MMP9-wt; indeed, MMP9-wt and MMP9-LDL xenografts showed comparable levels of active forms when analyzed by gelatin zymography (Fig. 5A).

To determine whether the enhanced angiogenesis in MMP9-wt-expressing tumors requires MMP9 activity, we injected MMP9-wt-expressing cells into mice treated with doxycycline, a potent MMP9 inhibitor of the tetracycline family (Sobrin et al., 2000). Doxycycline did not affect MMP9 levels in tumor extracts or sera of tumor-bearing mice (Fig. 6A); nevertheless, MMP9-wt-expressing tumors from doxycycline-treated mice showed a clear reduction in MMP9 activity (Fig. 6B). Concomitant with inhibition of MMP activity, doxycycline treatment reduced the average size (Fig. 6C) and growth kinetics (Fig. 6D) of MMP9-wt xenografts, but not of mock-transfected xenografts (Fig. S2, http://jcs.biologists.org/supplemental/). Moreover, microvessel density (Fig. 6E) and perimeter (Fig. 6F) were diminished in MMP9-wt tumors from doxycycline-treated mice. Inhibition of MMP activity thus abrogates the growth advantage and the increased angiogenesis in MMP9-wt-expressing tumors.

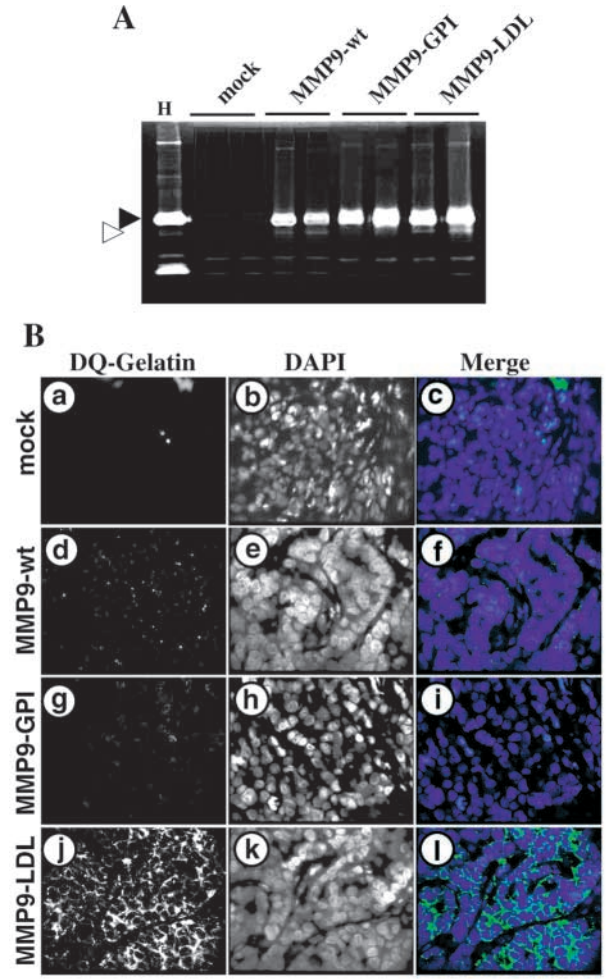

Fig. 5. Analysis of MMP9 in tumor xenografts. (A) Equal protein amounts of crude tumor extract were analyzed in gelatin zymography. Solid and open arrowheads indicate migration of proMMP9 and MMP9 forms, respectively, according to the activity detected in HT-1080 medium (H). (B) Tumor sections were incubated with DQ-gelatin (a,d,g,j; green in merged images) to detect in situ gelatinolytic activity; nuclei were stained with DAPI (b,e,h,k; blue in merged images). Magnification, ×400.

MMP9-wt expression specifically alters VEGF distribution

To determine the molecular basis of enhanced angiogenesis in MMP9-wt-expressing tumors, we measured levels of proangiogenic proteins in the tumor environment. No significant differences were found in human VEGF, TGFβ, bFGF, IL8 or mouse VEGF levels in extracts of any MMP9-expressing tumors (Table 1). Doxycycline did not affect VEGF levels (9.7±0.74 and 31.5±7.38 pg/100 μg tissue, for murine and human VEGF in tumors from doxycycline-treated animals, respectively).

MMP9 enhances angiogenesis by activating latent TGFβ through a mechanism that involves extracellular proteolytic degradation of the TGFβ latency-associated peptide (β-LAP) (Yu and Stamenkovic, 2000). Western blot analysis of mock-transfected or MMP9-expressing tumor extracts with anti-β1-LAP antibody showed a unique band of 40 kDa (not shown),

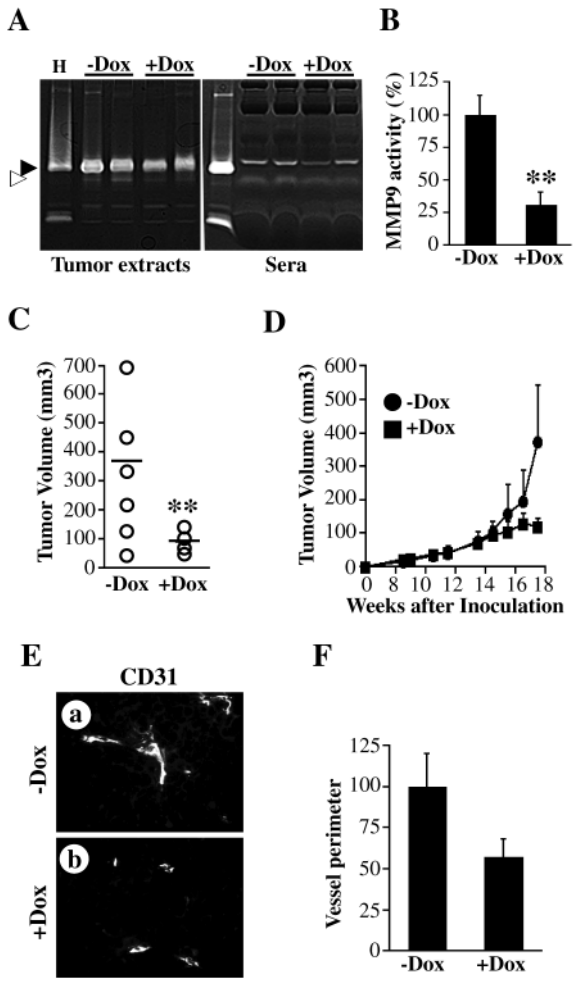

Fig. 6. Doxycycline abolishes MMP9-wt-enhanced tumor angiogenesis. (A) Gelatinolytic activity in crude tumor extracts (left) and sera (right) from untreated (–Dox) or doxycycline-treated mice (+Dox). Solid and open arrowheads indicate migration of proMMP9 and MMP9 forms, respectively, according to the activity detected in HT-1080 medium (H). (B) MMP9 activity was measured in tumor extracts using DQ-gelatin as substrate. Values represent the mean±s.e.m. obtained in triplicates of two samples per group. The value obtained in untreated samples was considered as 100% (**P<0.05). (C) Average tumor size at 17 weeks. The difference between –Dox (n=6) and +Dox (n=8) tumors was statistically significant (**P<0.05). (D) Tumor growth kinetics in the same mice as in C, over a 17-week period. Mean values±s.e.m. are represented. (E) Anti-CD31 staining of sections from tumors in –Dox and +Dox-treated mice. Magnification ×400. (F) Vascular perimeter estimated as the percentage of CD31-stained area. The value obtained for –Dox samples was considered as 100.

the expected molecular size for the monomer of non-proteolyzed β-LAP.

MMP9 may also release VEGF from ECM stores (Bergers et al., 2000). Immunohistochemical analysis with anti-VEGF antibodies demonstrated changes in VEGF distribution in MMP9-expressing tumors. The GV39M antibody, which specifically recognizes VEGF bound to VEGFR2 (Brekken et al., 1998), showed that VEGF complexed to VEGFR2 was more abundant in MMP9-wt-expressing tumors (Fig. 7Ae) than in mock-transfected (Fig. 7Ab), MMP9-GPI (Fig. 7Ah) or MMP9-LDL tumors (Fig. 7Ak); concurrently, CD31 stained more structures in MMP9-wt than in xenografts expressing other MMP forms (Fig. 7Aa,d,g,j). These tumors were anti-VEGFR2-stained (not shown) and the pattern was consistent with that of GV39M and CD31 reactivity. In contrast to receptor-bound VEGF, unbound VEGF appeared as diffuse staining, consistent with binding of this growth factor to ECM components (Fig. 7Ac,f,i,l). Receptor-bound VEGF was lower in MMP9-wt tumors from doxycycline-treated mice (Fig. 7Be) compared to those from untreated animals (Fig. 7Bb). These results strongly suggest that the change in VEGF distribution observed in MMP9-wt tumors is dependent on MMP9 activity.

Discussion

In this study, we generated a human breast cancer xenograft model using tumor cells overexpressing MMP9-wt and artificially membrane-anchored MMP9 forms. Targeting of MMP9 to non-raft membrane domains rendered a constitutive active MMP9 on the cell surface able to degrade two distinct substrates, DQ-gelatin and the fluorogenic M-2055 peptide. Using this model, we provide evidence that localization of this proteolytically active MMP9 chimera to the tumor membrane does not enhance invasive capacity, tumor growth kinetics or tumor-associated angiogenesis compared to mock-infected cells, which express very low MMP9 levels. Notwithstanding, all of these processes were significantly increased in tumor cells overexpressing the secreted MMP9 wild-type form, indicating a role for MMP9 in tumor progression.

The MMPs are synthesized as inactive zymogens that must be activated by proteolytic cleavage. Secreted MMP may be activated at the cell surface, as seen for proMMP-2 activation by MMP14 (Sato et al., 1994). MMP attachment to cell surface-bound matrix molecules may also protect against proteolytic activation, as reported in proMMP-2 binding to β1 integrin-bound collagen (Steffensen et al., 1998). MMP2 and MMP14 colocalization with caveolin-1 (Annabi et al., 2001; Puyraimond et al., 2001) suggested that compartmentalization

Table 1. Levels of angiogenic factors in tumor extracts

	mVEGF	hVEGF	bFGF	TGFβ	IL8
Mock	7.66±1.80	25.67±18.26	69.75±8.01	104.65±10.51	0.221±0.020
MMP9-wt	12.34±2.84	42.75±6.55	54.25±4.73	91.57±6.96	0.243±0.141
MMP9-GPI	8.73±1.80	36.17±13.30	53.33±6.48	75.39±10.02	0.296±0.061
MMP9-LDL	11.37±3.97	34.67±21.70	61.67±14.72	97.02±13.43	0.311±0.048

Values indicate the mean±s.e.m. (pg/100 μg of tumor extract) of three samples from each group of tumors.

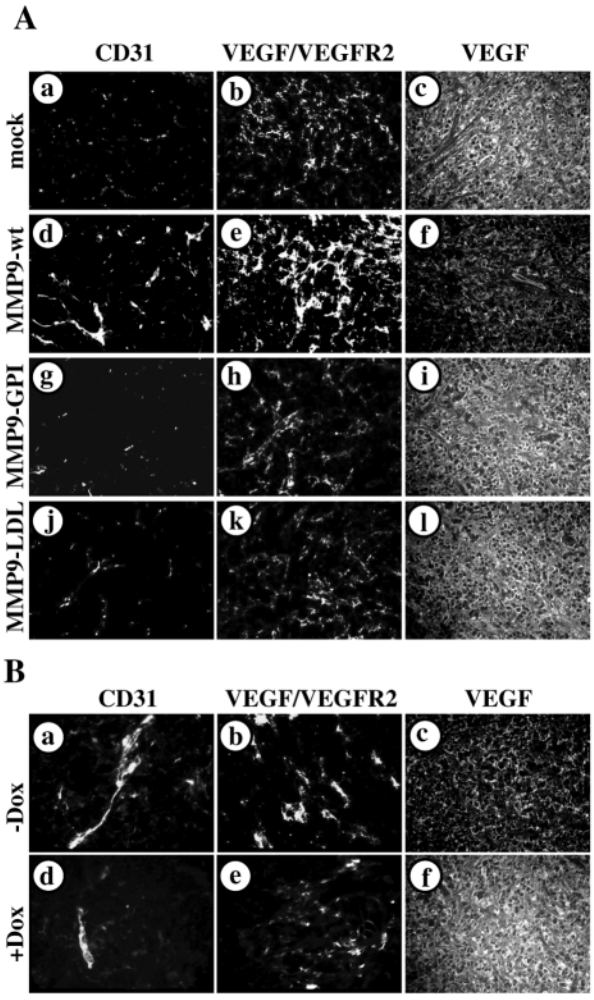

Fig. 7. VEGF distribution is specifically altered in tumors expressing soluble MMP9. (A) VEGF expression was evaluated in tumor sections using GV39M antibody, which recognizes VEGF bound to VEGFR2 (b,e,h,k), and an anti-VEGF mAb, which recognizes the receptor-free form (c,f,i,l). Sections were also stained with anti-CD31 for vessel identification (a,d,g,j). Magnification, ×200. (B) Sections from MMP9-wt tumors in untreated (–Dox, a-c) or doxycycline-treated (+Dox, d-f) mice were stained as in A. Magnification, ×200.

of MMP precursors and activators to specific membrane subdomains may be important in regulating zymogen activation. Our results concur with this observation, as we found a differential activation pattern by targeting MMP9 to raft or non-raft domains in two cell lines. However, both MMP9 chimeras are processed similarly by chemical activators, suggesting that the processing differences are due to their partitioning to raft and non-raft domains rather than to constraints imposed by the tags that target MMP9 to the membrane.

MMP inhibitors blocked constitutive activation of non-raft MMP9. This suggests the involvement of other non-raft MMPs or autoactivation of non-raft MMP9, consistent with the view that some MMPs initiate or maintain their activation (Nagase, 1997). According to this hypothesis, homotypic interactions leading to autoactivation might be favored when MMP9 partitions in a non-ordered membrane environment (non-raft) and restricted when it is targeted to liquid-ordered rafts. Lack of raft-targeted proMMP9 autoactivation may also be caused by concentration of specific MMP9 inhibitors in rafts; the GPI-anchored RECK is a potential inhibitor candidate. We nonetheless did not detect RECK expression in MCF-7 or DU-145 cells (not shown). In addition, it is not known how these MMP9 chimeras interact with tissue inhibitor of metalloproteases (TIMPs).

The differences in activation between raft- and non-raft-targeted MMP9 may have implications in cell migration. At the single cell level, migration involves coordinated, dynamic interplay of attachment at the cell front (leading edge) and detachment at the rear cell edge (Mañes et al., 2000). Cell movement is initiated by lamellipodial and/or filopodial extensions at the leading edge, which must be stabilized by attachment to the ECM substrate. Formation of adhesion sites at the leading edge allows the generation of traction forces by myosin-based contraction, which pushes the cell body forward; release of the rear cell edge from the substrate completes the cycle. As rafts accumulate asymmetrically at the leading edge of moving epithelial and mesenchymal cells (Mañes et al., 1999b; Zhao et al., 2002; Mañes et al., 2003a), MMP inclusion in these domains may be a mechanism to silence local MMP activity at the cell front, where adhesion to the ECM must stabilize invadopodia. The rear of these cells is largely devoid of rafts, and MMP-mediated ECM degradation can proceed. Concurring with this view, smooth muscle cell migration requires the localized activity of membrane-bound MMP1 at the rear cell edge (Li et al., 2000). Regulation of proteolysis by raft/non-raft association may be more complex; for example, lymphocytes have two distinct raft subtypes that segregate to cell poles during migration (Gómez-Moutón et al., 2001).

An important observation of this study is that tumors grow more rapidly when MMP9 is secreted to the pericellular environment than when it remains anchored to the tumor cell surface. Upregulation of secreted MMP9 correlated with an increase in tumor growth kinetics and angiogenesis compared to cells expressing low MMP9 levels (mock) or active MMP9 on the tumor cell surface (MMP9-LDL). This enhancement was partially inhibited by doxycycline, indicating that these effects require the proteolytic activity of the secreted MMP9 form. We ruled out the use of TIMP1-transfected cells to inhibit MMP9 activity, as this inhibitor upregulates proangiogenic VEGF expression and increases MCF-7 cell proliferation (Yoshiji et al., 1998).

MMP9 is implicated in regulating tumor angiogenesis via a mechanism that involves VEGF release from ECM stores (Bergers et al., 2000; Rodríguez-Manzaneque et al., 2001). Using antibodies specific for the VEGF/VEGFR2 complex (Brekken et al., 1998), we found VEGF distribution differences that correlate with MMP9 location. VEGF/VEGFR2 complex was significantly increased in xenografts producing secreted MMP9, and this increase was dependent on MMP9 proteolytic activity. The molecular mechanism by which secreted MMP9 enhances angiogenesis may thus involve the generation of ‘bioactive’ VEGF. Whether VEGF release is caused by free MMP9 or requires interaction of secreted MMP9 with stromal components, including association to the stromal cell plasma membrane, warrants future research. In situ zymography

suggests that MMP9-wt is unlikely to be more efficient than the constitutive active non-raft MMP9 forms in remodeling ECM. We cannot rule out the possibility that the non-MMP9 chimera, although able to proteolyze DQ-gelatin, is unable to degrade other substrates. We nonetheless favor the hypothesis that secreted MMP9 spatially controls VEGF release from ECM stores.

Studies using MMP9-deficient mice suggested that host inflammatory cells that invade tumors are the critical suppliers of MMP9, which promotes tumor growth, invasion and the angiogenic switch (Bergers et al., 2000; Coussens et al., 2000; Hiratsuka et al., 2002). In another human xenograft model, growth and angiogenesis were independent of tumor cell MMP9 expression, but required MMP9 production by host inflammatory cells (Huang et al., 2002). These results suggest that MMP9 functions as a paracrine regulator of tumor progression; the data from our non-raft MMP9 chimera support this concept.

Another intriguing possibility is that constitutive localization of active MMP9 on the tumor cell surface might create a microenvironment unfavorable for tumor progression. MMP9 is implicated in the generation of molecules with antiangiogenic activity (Patterson and Sang, 1997; Stetler-Stevenson, 1999; Pozzi et al., 2002). Angiogenesis defects in RECK-deficient mice suggested that excess proteolysis is detrimental, yet excessive proteolytic inhibition by RECK overexpression in tumor cells also impairs angiogenesis (Oh et al., 2001). Local overstimulation of the plasminogen activation system also impairs angiogenesis, leading to the concept that increased proteolysis in restricted areas may be a strategy to halt tumor progression (Reijerkerk et al., 2000). Although tumor formation is somewhat delayed in cells expressing activated non-raft MMP9, we observed no severe detrimental effect from constitutive active MMP9 expression in MCF-7 cells compared to mock-transfected cells. The non-raft MMP9 chimera may nonetheless be a useful tool for analyzing the effect of excess proteolysis in other tumor models.

In summary, in this model we show that location of an active MMP9 chimera on the tumor cell surface does not accelerate tumor progression. These results do not diminish the role of the plasma membrane in the regulation of MMP9 activity; however, they stress that the balance between MMP activity and its physical location probably determines the efficiency of ECM remodeling, leading to angiogenesis and invasion. Comprehension of the regulatory mechanisms that restrict MMP activity in specific locations may open new avenues for therapeutic intervention.

We thank C. López-Otín for critical reading of manuscript, R. A. Brekken and P. E. Thorpe for the kind gift of the GV39M monoclonal antibody, F. Colotta for BB-94, L. Gómez for help with animal work, M. C. Moreno-Ortiz for flow cytometry, F. Ortego for statistical analysis, and C. Mark for editorial assistance. S.J.B. is the recipient of a predoctoral fellowship from the Spanish Ministerio de Ciencia y Tecnología. The Department of Immunology and Oncology was founded and is supported by the Spanish Council for Scientific Research (CSIC) and by Pfizer.

References

Annabi, B., Lachambre, M., Bousquet-Gagnon, N., Page, M., Gingras, D. and Beliveau, R. (2001). Localization of membrane-type 1 matrix metalloproteinase in caveolae membrane domains. *Biochem. J.* **353**, 547-553.

Bergers, G., Brekken, R., McMahon, G., Vu, T., Itoh, T., Tamaki, K., Tanzawa, K., Thorpe, P., Itohara, S., Werb, Z. et al. (2000). Matrix metalloproteinase-9 triggers the angiogenic switch during carcinogenesis. *Nat. Cell Biol.* **2**, 737-744.

Bourguignon, L., Gunja-Smith, Z., Iida, N., Zhu, H., Young, L., Muller, W. and Cardiff, R. (1998). CD44v(3,8-10) is involved in cytoskeleton-mediated tumor cell migration and matrix metalloproteinase (MMP-9) association in metastatic breast cancer cells. *J. Cell Physiol.* **176**, 206-215.

Brekken, R., Huang, X., King, S. and Thorpe, P. (1998). Vascular endothelial growth factor as a marker of tumor endothelium. *Cancer Res.* **58**, 1952-1959.

Brooks, P., Stromblad, S., Sanders, L., von Schalscha, T., Aimes, R., Stetler-Stevenson, W., Quigley, J. and Cheresh, D. (1996). Localization of matrix metalloproteinase MMP-2 to the surface of invasive cells by interaction with integrin alpha v beta 3. *Cell* **85**, 683-693.

Coussens, L., Tinkle, C., Hanahan, D. and Werb, Z. (2000). MMP-9 supplied by bone marrow-derived cells contributes to skin carcinogenesis. *Cell*. **103**, 481-490.

del Real, G., Jiménez-Baranda, S., Lacalle, R. A., Mira, E., Lucas, P., Gómez-Moutón, C., Carrera, A., Martínez-A, C. and Mañes, S. (2002). Blocking of HIV-1 infection by targeting CD4 to nonraft membrane domains. *J. Exp. Med.* **196**, 293-301.

Egeblad, M. and Werb, Z. (2002). New functions for the matrix metalloproteinases in cancer progression. *Nat. Rev. Cancer*. **2**, 161-174.

Fingleton, B., Vargo-Gogola, T., Crawford, H. and Matrisian, L. (2001). Matrilysin [MMP-7] expression selects for cells with reduced sensitivity to apoptosis. *Neoplasia* **3**, 459-468.

Fiore, E., Fusco, C., Romero, P. and Stamenkovic, I. (2002). Matrix metalloproteinase 9 (MMP-9/gelatinase B) proteolytically cleaves ICAM-1 and participates in tumor cell resistance to natural killer cell-mediated cytotoxicity. *Oncogene*, **21**, 5213-5223.

Fridman, R. (2003). Surface association of secreted matrix metalloproteinases. *Curr. Top. Dev. Biol.* **54**, 75-100.

Gómez-Moutón, C., Abad, J. L., Mira, E., Lacalle, R. A., Gallardo, E., Jiménez-Baranda, S., Illa, I., Bernad, A., Mañes, S. and Martínez-A, C. (2001). Segregation of leading-edge and uropod components into specific lipid rafts during T cell polarization. *Proc. Natl. Acad. Sci. USA* **98**, 9642-9647.

Guo, H., Li, R., Zucker, S. and Toole, B. (2000). EMMPRIN (CD147), an inducer of matrix metalloproteinase synthesis, also binds interstitial collagenase to the tumor cell surface. *Cancer Res.* **60**, 888-891.

Hahn-Dantona, E., Ruiz, J., Bornstein, P. and Strickland, D. (2001). The low density lipoprotein receptor-related protein modulates levels of matrix metalloproteinase 9 (MMP-9) by mediating its cellular catabolism. *J. Biol. Chem.* **276**, 15498-15503.

Hiratsuka, S., Nakamura, K., Iwai, S., Murakami, M., Itoh, T., Kijima, H., Shipley, J., Senior, R. and Shibuya, M. (2002). MMP9 induction by vascular endothelial growth factor receptor-1 is involved in lung-specific metastasis. *Cancer Cell*. **2**, 289-300.

Huang, S., van Arsdall, M., Tedjarati, S., McCarthy, M., Wu, W., Langley, R. and Fidler, I. (2002). Contributions of stromal metalloproteinase-9 to angiogenesis and growth of human ovarian carcinoma in mice. *J. Natl. Cancer Inst.* **94**, 1134-1142.

Kim, J., Yu, W., Kovalski, K. and Ossowski, L. (1998). Requirement for specific proteases in cancer cell intravasation as revealed by a novel semiquantitative PCR-based assay. *Cell* **94**, 353-362.

Li, S., Chow, L. and Pickering, J. (2000). Cell surface-bound collagenase-1 and focal substrate degradation stimulate the rear release of motile vascular smooth muscle cells. *J. Biol. Chem.* **275**, 35384-35392.

Mañes, S., Mira, E., Barbacid, M., Ciprés, A., Fernández-Resa, P., Buesa, J., Mérida, I., Aracil, M., Márquez, G. and Martínez-A, C. (1997). Identification of insulin-like growth factor-binding protein-1 as a potential physiological substrate for human stromelysin-3. *J. Biol. Chem.* **272**, 25706-25712.

Mañes, S., Llorente, M., Lacalle, R. A., Gómez-Moutón, C., Kremer, L., Mira, E. and Martínez-A, C. (1999a). The matrix metalloproteinase-9 regulates the insulin-like growth factor-triggered autocrine response in DU-145 carcinoma cells. *J. Biol. Chem.* **274**, 6935-6945.

Mañes, S., Mira, E., Gómez-Moutón, C., Lacalle, R. A., Keller, P., Labrador, J. and Martínez-A, C. (1999b). Membrane raft microdomains mediate front-rear polarity in migrating cells. *EMBO J.* **18**, 6211-6220.

Mañes, S., Mira, E., Gómez-Moutón, C., Lacalle, R. A. and Martínez-A,

C. (2000). Cells on the move: a dialogue between polarization and motility. *IUBMB Life* **49**, 89-96.

Mañes, S., Lacalle, R. A., Gómez-Moutón, C., del Real, G., Mira, E. and Martínez-A, C. (2001). Membrane raft microdomains in chemokine receptor function. *Semin. Immunol.* **13**, 143-157.

Mañes, S., Lacalle, R. A., Gómez-Moutón, C. and Martínez-A, C. (2003a). From rafts to crafts: membrane asymmetry in moving cells. *Trends Immunol.* **24**, 319-325.

Mañes, S., del Real, G. and Martínez-A, C. (2003b). Pathogens: raft hijackers. *Nat. Rev. Immunol.* **3**, 557–568.

Mazzieri, R., Masiero, L., Zanetta, L., Monea, S., Onisto, M., Garbisa, S. and Mignatti, P. (1997). Control of type IV collagenase activity by components of the urokinase-plasmin system: a regulatory mechanism with cell-bound reactants. *EMBO J.* **16**, 2319-2332.

McQuibban, G., Gong, J., Tam, E., McCulloch, C., Clark-Lewis, I. and Overall, C. (2000). Inflammation dampened by gelatinase A cleavage of monocyte chemoattractant protein-3. *Science* **289**, 1202-1206.

McQuibban, G., Gong, J., Wong, J., Wallace, J., Clark-Lewis, I. and Overall, C. (2002). Matrix metalloproteinase processing of monocyte chemoattractant proteins generates CC chemokine receptor antagonists with anti-inflammatory properties in vivo. *Blood* **100**, 1160-1167.

Mira, E., Mañes, S., Lacalle, R. A., Márquez, G. and Martínez-A, C. (1999). Insulin-like growth factor I-triggered cell migration and invasion are mediated by matrix metalloproteinase-9. *Endocrinology* **140**, 1657-1664.

Mira, E., Lacalle, R. A., González, M. A., Gómez-Moutón, C., Abad, J. L., Bernad, A., Martínez-A, C. and Mañes, S. (2001). A role for chemokine receptor transactivation in growth factor signaling. *EMBO Rep.* **2**, 151-156.

Mira, E., Lacalle, R. A., Gómez-Moutón, C., Leonardo, E. and Mañes, S. (2002). Quantitative determination of tumor cell intravasation in a real-time polymerase chain reaction-based assay. *Clin. Exp. Metastasis* **19**, 313-318.

Mori, H., Tomari, T., Koshikawa, N., Kajita, M., Itoh, Y., Sato, H., Tojo, H., Yana, I. and Seiki, M. (2002). CD44 directs membrane-type 1 matrix metalloproteinase to lamellipodia by associating with its hemopexin-like domain. *EMBO J.* **21**, 3949-3959.

Nagase, H. (1997). Activation mechanisms of matrix metalloproteinases. *Biol. Chem.* **378**, 151-160.

Oh, J., Takahashi, R., Kondo, S., Mizoguchi, A., Adachi, E., Sasahara, R., Nishimura, S., Imamura, Y., Kitayama, H., Alexander, D. et al. (2001). The membrane-anchored MMP inhibitor RECK is a key regulator of extracellular matrix integrity and angiogenesis. *Cell* **107**, 789-800.

Olson, M., Toth, M., Gervasi, D., Sado, Y., Ninomiya, Y. and Fridman, R. (1998). High affinity binding of latent matrix metalloproteinase-9 to the alpha2(IV) chain of collagen IV. *J. Biol. Chem.* **273**, 10672-10681.

Overall, C. and López-Otín, C. (2002). Strategies for MMP inhibition in cancer: innovations for the post-trial era. *Nat. Rev. Cancer*, **2**, 657-672.

Partridge, C., Phillips, P., Niedbala, M. and Jeffrey, J. (1997). Localization and activation of type IV collagenase/gelatinase at endothelial focal contacts. *Am. J. Physiol.* **272**, L813-L822.

Patterson, B. and Sang, Q. (1997). Angiostatin-converting enzyme activities of human matrilysin (MMP-7) and gelatinase B/type IV collagenase (MMP-9). *J. Biol. Chem.* **272**, 28823-28825.

Pozzi, A., LeVine, W. and Gardner, H. (2002). Low plasma levels of matrix metalloproteinase 9 permit increased tumor angiogenesis. *Oncogene* **21**, 272-281.

Puyraimond, A., Fridman, R., Lemesle, M., Arbeille, B. and Menashi, S. (2001). MMP-2 colocalizes with caveolae on the surface of endothelial cells. *Exp. Cell Res.* **262**, 28-36.

Quesada, A., Barbacid, M., Mira, E., Fernández-Resa, P., Márquez, G. and Aracil, M. (1997). Evaluation of fluorometric and zymographic methods as activity assays for stromelysins and gelatinases. *Clin. Exp. Metastasis* **15**, 26-32.

Ramos-DeSimone, N., Hahn-Dantona, E., Sipley, J., Nagase, H., French, D. and Quigley, J. (1999). Activation of matrix metalloprotease-9 (MMP-9) via a converting Plasmin/Stromelysin-1 cascade enhances tumor cell invasion. *J. Biol. Chem.* **274**, 13066-13076.

Reijerkerk, A., Voest, E. and Gebbink, M. (2000). No grip, no growth: the conceptual basis of excessive proteolysis in the treatment of cancer. *Eur. J. Cancer* **36**, 1695-1705.

Rodríguez-Manzaneque, J., Lane, T., Ortega, M., Hynes, R., Lawler, J. and Iruela-Arispe, M. (2001). Thrombospondin-1 suppresses spontaneous tumor growth and inhibits activation of matrix metalloproteinase-9 and mobilization of vascular endothelial growth factor. *Proc. Natl. Acad. Sci. USA* **98**, 12485-12490.

Sato, H., Takino, T., Okada, Y., Cao, J., Shinagawa, A., Yamamoto, E. and Seiki, M. (1994). A matrix metalloproteinase expressed on the surface of invasive tumour cells. *Nature*, **370**, 61-65.

Simons, K. and Toomre, D. (2000). Lipid rafts and signal transduction. *Nat. Rev. Mol. Cell. Biol.* **1**, 31-39.

Sobrin, L., Liu, Z., Monroy, D., Solomon, A., Selzer, M., Lokeshwar, B. and Pflugfelder, S. (2000). Regulation of MMP-9 activity in human tear fluid and corneal epithelial culture supernatant. *Invest. Ophthalmol. Vis. Sci.* **41**, 1703-1709.

Steffensen, B., Bigg, H. and C. Overall, C. (1998). The involvement of the fibronectin type II-like modules of human gelatinase A in cell surface localization and activation. *J. Biol. Chem.* **273**, 20622-20628.

Stetler-Stevenson, W. (1999). Matrix metalloproteinases in angiogenesis: a moving target for therapeutic intervention. *J. Clin. Invest.* **103**, 1237-1241.

Toth, M., Sado, Y., Ninomiya, Y. and Fridman, R. (1999). Biosynthesis of alpha2(IV) and alpha1(IV) chains of collagen IV and interactions with matrix metalloproteinase-9. *J. Cell Physiol.* **180**, 131-139.

Wilson, C., Ouellette, A., Satchell, D., Ayabe, T., López-Boado, Y., Stratman, J., Hultgren, S., Matrisian, L. and Parks, W. (1999). Regulation of intestinal alpha-defensin activation by the metalloproteinase matrilysin in innate host defense. *Science* **286**, 113-117.

Yoshiji, H., Harris, S., Raso, E., Gómez, D., Lindsay, C., Shibuya, M., Sinha, C. and Thorgeirsson, U. (1998). Mammary carcinoma cells over-expressing tissue inhibitor of metalloproteinases-1 show enhanced vascular endothelial growth factor expression. *Int. J. Cancer* **75**, 81-87.

Yu, Q. and Stamenkovic, I. (2000). Cell surface-localized matrix-metalloproteinase-9 proteolytically activates TGF-β and promotes tumor invasion and angiogenesis. *Genes Dev.* **14**, 163-176.

Yu, W. and Woessner, J. (2000). Heparan sulfate proteoglycans as extracellular docking molecules for matrilysin (matrix metalloproteinase 7). *J. Biol. Chem.* **275**, 4183-4191.

Zhao, M., Pu, J., Forrester, J. and McCaig, C. (2002). Membrane lipids, EGF receptors, and intracellular signals colocalize and are polarized in epithelial cells moving directionally in a physiological electric field. *FASEB J.* **16**, 857-859.

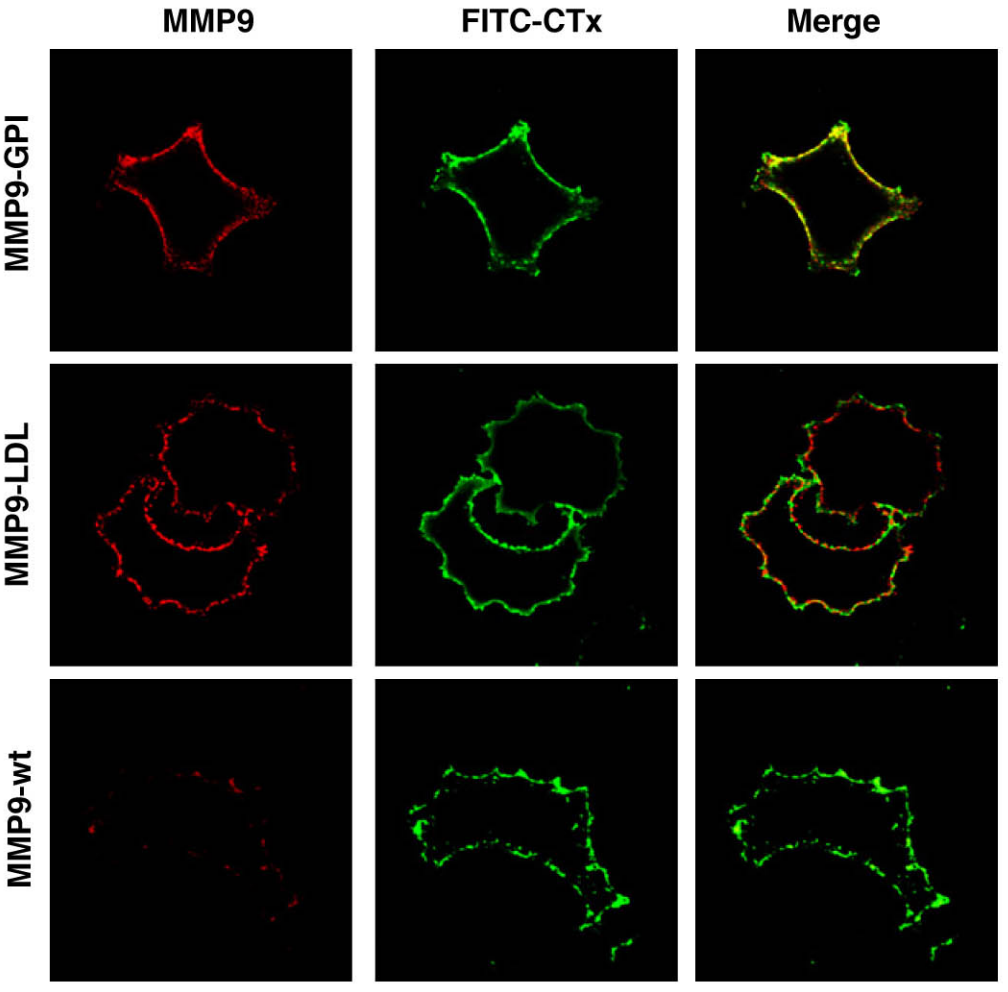

Mira et al.,
Suppl. Fig 1S

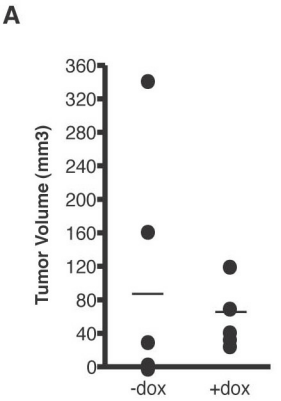

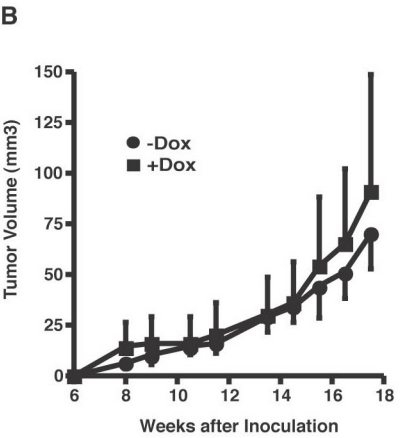

Mira et al.,
Figure 2S